Supplementary Material for

Extremely Efficient Terahertz Second-Harmonic Generation from Organic Crystals

Authors

Hang Zhao,[a,b,†] Yong Tan,[c,d,e,†] Chen Wang,[c] Ming Liu,[a,b] Yongzheng Wen,[c,*] Yuejin Zhao,[a,b,f,*] Ji Zhou[c,*]

Affiliations

[a]Beijing Key Laboratory for Precision Optoelectronic Measurement Instrument and Technology, School of Optics and Photonics, Beijing Institute of Technology, Beijing 100081, China;

[b]Yangtze Delta Region Academy of Beijing Institute of Technology, Jiaxing 314019, China;

[c]State Key Laboratory of New Ceramics and Fine Processing, School of Materials Science and Engineering, Tsinghua University, Beijing 100084, China;

[d]Research Center for Metamaterials, Wuzhen Laboratory, Jiaxing 314500, China;

[e]Advanced Ceramic Materials and Devices Research Center, Yangtze Delta Region Institute of Tsinghua University, Jiaxing 314000, China

[f]Beijing Broad Hengtong Technology Development Co. Ltd, Beijing 102600, China

†These authors contributed equally to this work.

*Correspondence: Yongzheng Wen (wenyzheng@tsinghua.edu.cn), Yuejin Zhao (yjzhao@bit.edu.cn), and Ji Zhou (zhouji@tsinghua.edu.cn)

Supplementary Material

SI. Experimental setup and correction of the measured electric field

Our experimental system is shown in Fig. S1. The laser produced by a Ti: sapphire laser system (Coherent, Astrella) with a central wavelength of 800 nm (repetition rate of 1 kHz, pulse duration of 35 fs, pulse energy of 7 mJ) is separated into two beams by a beam splitter with a 5:5 (R:T) split ratio. One of the 3.5 mJ beams is used to pump a commercial optical parametric amplifier (OPA, Coherent, Opera Solo), which delivers an optical laser beam with a wavelength of 1550 nm (repetition rate of 1 kHz, pulse duration of 35 fs, pulse energy of 450 μJ, bandwidth of 100 nm). The other beam is used as a probe laser with a wavelength of *y*-polarized 800 nm. The organic crystal (Crystal1) is pumped by the *x*-polarized 1550 nm femtosecond laser delivered by the OPA to generate incident broadband terahertz (THz) waves. The generated *x*-polarized THz wave is collected by a parabolic mirror (PM1, focal length of 1 inch) and recollimated by the PM2 (focal length of 6 inches), and then focused by PM3 (focal length of 2 inches) to reduce the size of the THz focal spot and achieve a strong THz field strength. Organic crystals used to generate second harmonics are placed at the THz focal position after PM3. Second harmonic pulse is generated in a focusing geometry, which can effectively achieve greater conversion efficiency and more accurate measurements of second-order nonlinear susceptibility. Three low-pass filters with a cutoff frequency of 18 THz were used to filter out the residual NIR spectrum. The energy of the THz wave is controlled by the THz polarizers (TPs). The directions of TP1 and TP3 in Fig. S1 are always along the *x*-direction, where TP1 guarantees that the degree of polarization of the THz wave closer to 1, and the THz power is controlled by adjusting the angle of TP2.

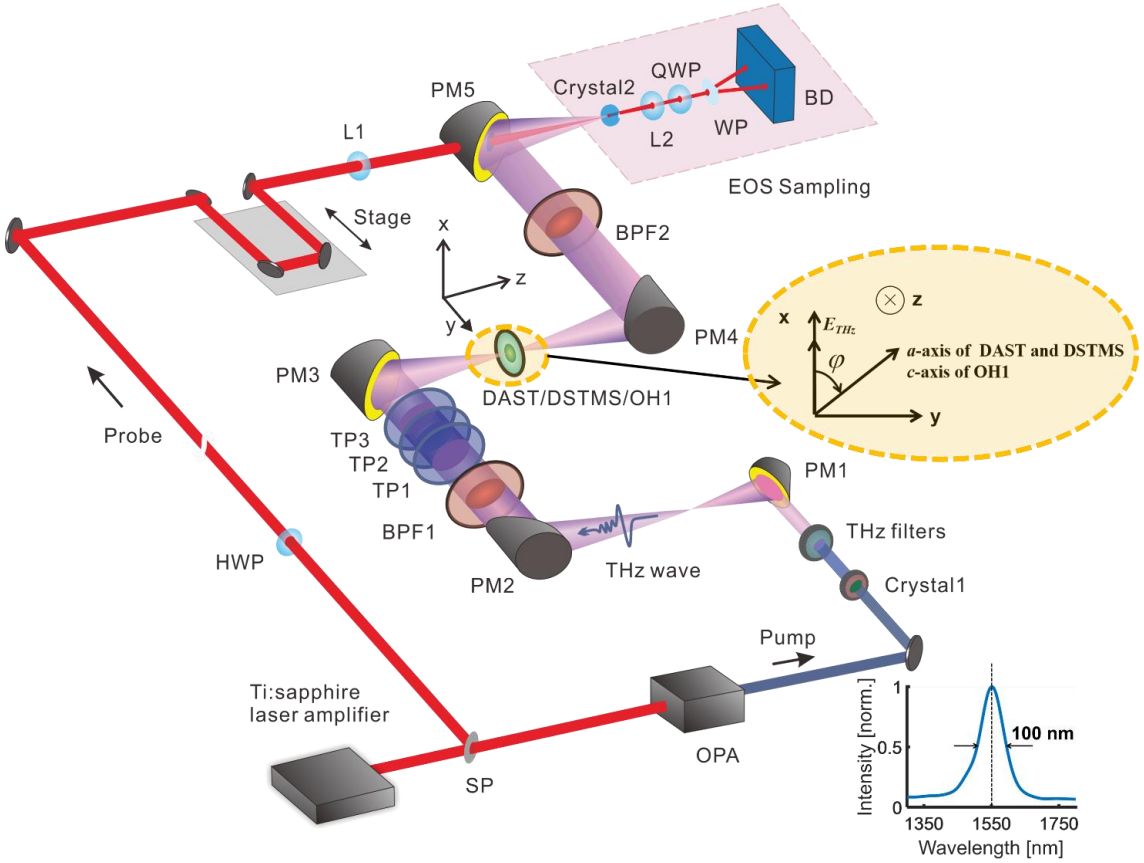

Fig. S1 Experimental setup for THz SHG measurement. SP: spliter; OPA: optical parametric amplifier (The inset shows the spectrum of 1550 nm signal); Crystal1: OH1/DAST crystal; THz filter: low-pass filters with the cut-off frequency of 18 THz; PM: parabolic mirror; BPF1: a pair of THz bandpass filters to efficiently extract a THz fundamental pulse with frequency of 2.4/1.6/0.8 THz ; TP: THz polarizer; BPF2: a pair of THz bandpass filters to extract the corresponding SHG with frequency of 4.8/3.2/1.6 THz; HWP: half-wave plate; L: optical lens; Crystal2: ZnTe/GaP crystal; QWP: quarter wave plate; WP: Wollaston prism; BD: Balance detector. The inset with yellow background shows the angle φ between the THz polarization direction and the crystal axis.

To improve the measurement accuracy, we use a pair of THz bandpass filters (BPF1) centered at 2.4/1.6/0.8 THz to efficiently extract a narrowband, multi-period quasi-monochromatic THz pulse, which is focused on a crystal without a substrate to induce second-order nonlinear effects. This pair of bandpass filters can be selected from products with the center frequency of 2.4 THz (Tydex, BP2400), 1.6 THz (Tydex, BP1600), or 0.8 THz (Tydex, BP0800). The peak field strengths of the THz pump pulse at different frequencies of 2.4 THz,1.6 THz, and 0.8 THz are 210.3 kV/cm, 78.6 kV/cm, and 23.5 kV/cm (as shown in the lower panel of Figs. 1 (b)-(d)),

corresponding to the peak intensities of 5.87×10^7 W/cm^2, 8.20×10^6 W/cm^2, 7.33×10^5 W/cm^2, respectively. We use a pair of THz bandpass filters (BPF2) centered at 4.8/3.2/1.6 THz to attenuate the fundamental field of the THz pulse passing through the crystal and extract the corresponding second harmonic generation (SHG). This pair of bandpass filters can be selected from products with the center frequency of 4.8 THz (Tydex, BP4800), 3.2 THz (Tydex, BP3200) or 1.6 THz (Tydex, BP1600). The 800 nm probe pulse is collinearly focused with the THz pulse onto the detection crystal for electro-optical sampling (EOS). Without applying a THz electric field, rotating the quarter wave plate (QWP) allows the probe pulse to be controlled as circular polarization after passing through the lens L2 and the QWP, thus compensating for the weak interference that the lens L2 may have on the polarization of the probe pulse. To eliminate the absorption of water vapor, the relative humidity of all measurements was maintained below 5% by purging with dry N_2 at room temperature.

The THz source (Crystal1 in Fig. S1) is selected as OH1 or DAST crystal, and the generated time-domain waveform and corresponding spectrum are shown in Fig. S2(a) and Fig. S2(b). The THz wave from OH1 is filtered with different THz filters to obtain the 1.6 THz and 0.8 THz pump pulse under the same condition, while the 2.4 THz pump pulse is filtered from the THz waves generated by the DAST crystal. For the THz detection (Crystal2 in Fig. S1), we use ZnTe crystal with a thickness of 1 mm to detect incident fundamental waves of 0.8 THz and corresponding second harmonic waves with 1.6 THz. For the incident fundamental waves of 2.4/1.6 THz and the corresponding second harmonic wave of 4.8/3.2 THz, GaP crystal with a thickness of 0.2 mm is used for detection. Because strong THz electric fields will saturate the signals detected by GaP and ZnTe crystals, the original field strength of THz waves cannot be measured directly. To ensure that the pump fundamental pulse and corresponding second harmonics can be within the dynamic response range of GaP/ZnTe at the same time, the pump THz electric field using THz polarizers and attenuator is reduced to 1% of the original.

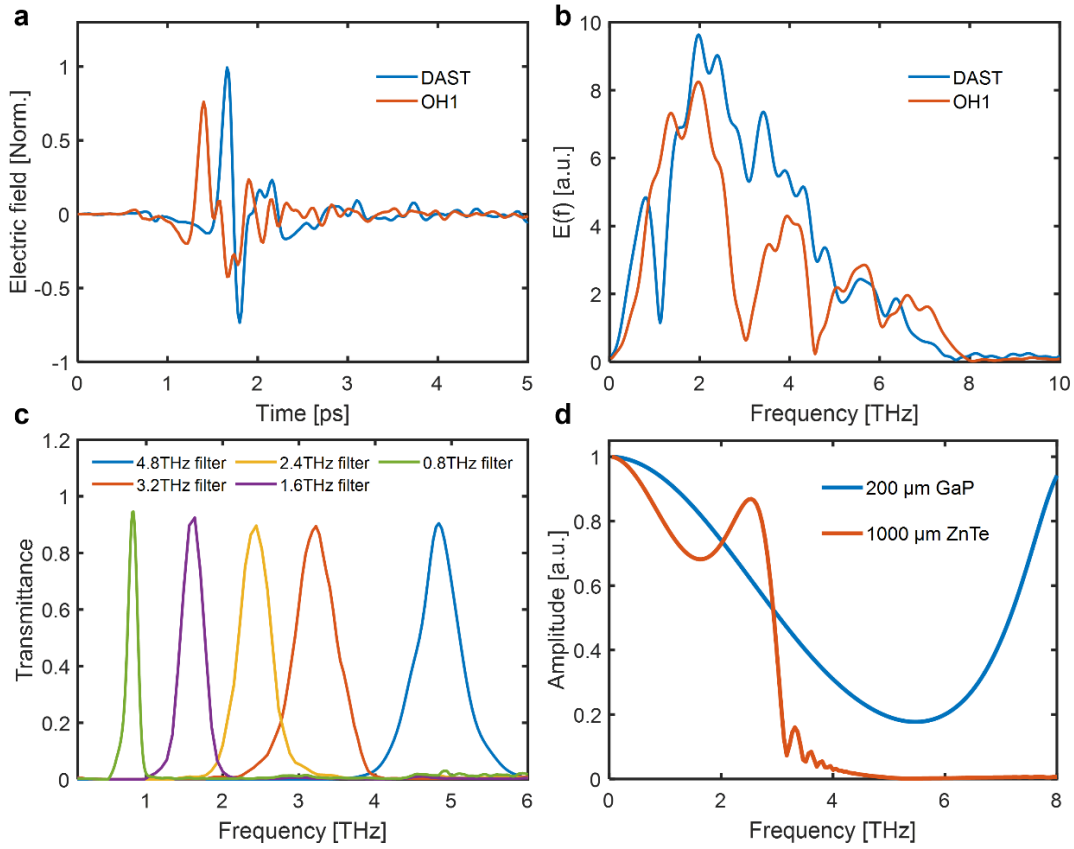

Fig. S2 (a) The time-domain waveform and (b) the spectrum of the broadband THz signal generated in OH1 and DAST crystals under the same experimental conditions. (c) The transmittance of different types of THz bandpass filters. (d) The frequency response functions of the GaP and ZnTe crystals.

Then, we use a THz camera to record the beam spot size at the THz focus, and measure the THz pulse energy with a pyroelectric detector. These are combined with the THz time-domain waveform to quantify the peak electric field strength. Specifically, for narrow-band THz pulses at 2.4 THz, 1.6 THz, and 0.8 THz, the beam spot areas measured by a THz camera are approximately 7.125×10^{-4} cm^2, 1.044×10^{-3} cm^2 and 2.275×10^{-3} cm^2, respectively. The pulse energies measured by a pyroelectric detector are 6.28×10^{-8} J, 1.91×10^{-8} J, and 7.5×10^{-9} J, respectively (after correction by attenuation factor), and the pulse widths measured by EOS method are 1.5 ps, 2.23 ps, and 4.47 ps, respectively. Therefore, we can evaluate that the peak electric field strengths of THz pump pulses at 2.4 THz, 1.6 THz, and 0.8 THz are 210.3 kV/cm, 78.6 kV/cm, and 23.5 kV/cm, respectively. In addition, the conversion efficiencies for SHG are corrected by the transmittance of the THz filter (Fig. S2(c))

and the response function of the GaP/ZnTe crystal (Fig. S2(d)).[39] The measured THz time-domain waveform of the pump pulse, as well as the SHG of the three crystals, are shown in Fig. S3. Moreover, the bandwidths of the SHG spectra from DAST, DSTMS, and OH1 shown in Fig. 1(e) are 0.51 THz, 0.50 THz, and 0.6 THz, respectively. The bandwidths of the SHG spectra from DAST, DSTMS, and OH1 shown in Fig. 1(f) are 0.33 THz, 0.32 THz, and 0.34 THz, respectively. The bandwidths of the SHG spectra from DAST, DSTMS, and OH1 shown in Fig. 1(g) are 0.15 THz, 0.13 THz, and 0.16 THz, respectively.

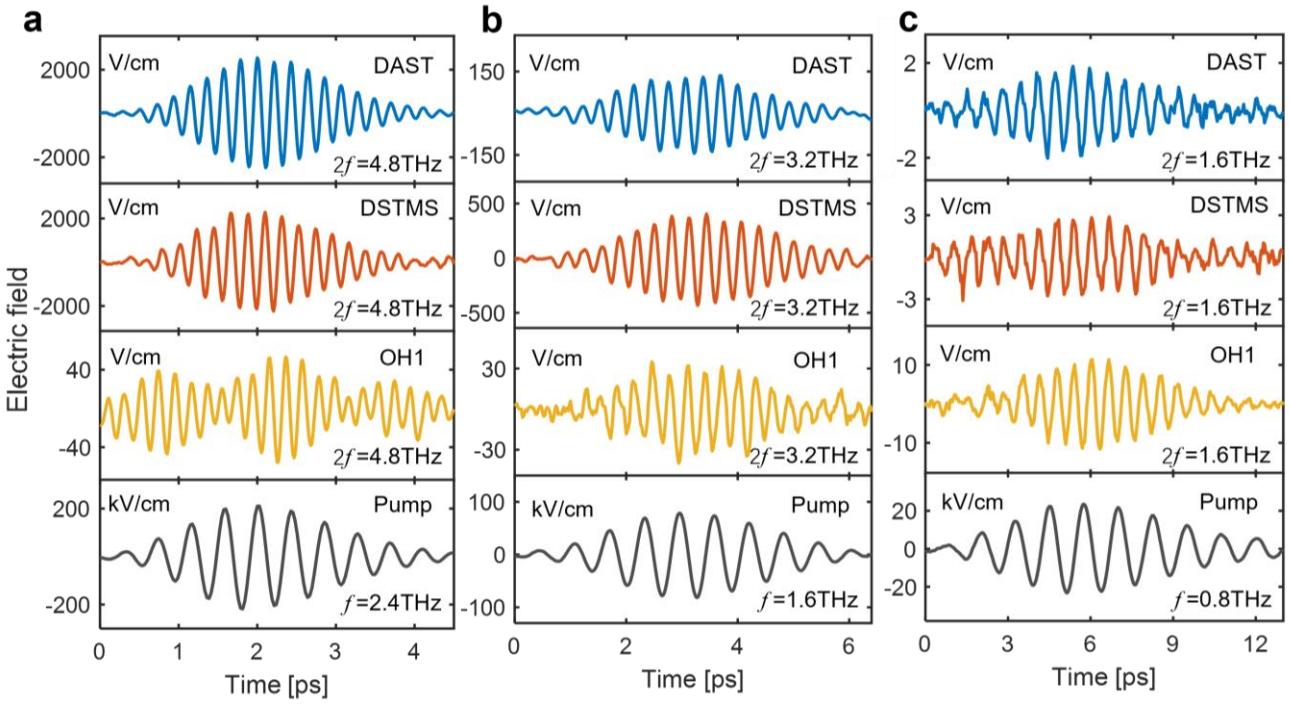

Fig. S3 THz SHG from organic crystals. (a)-(c) The time-domain waveform of THz SHG from different crystals with fundamental frequencies of 2.4 THz, 1.6 THz, and 0.8 THz.

SII. Optical properties of crystals in the THz range

Considering the number of resonant features of different crystals,[37,41-45] we use the Lorentz model to simulate the refractive index and absorption coefficient of DAST, DSTMS, and OH1 crystals, as shown in Fig. S4.

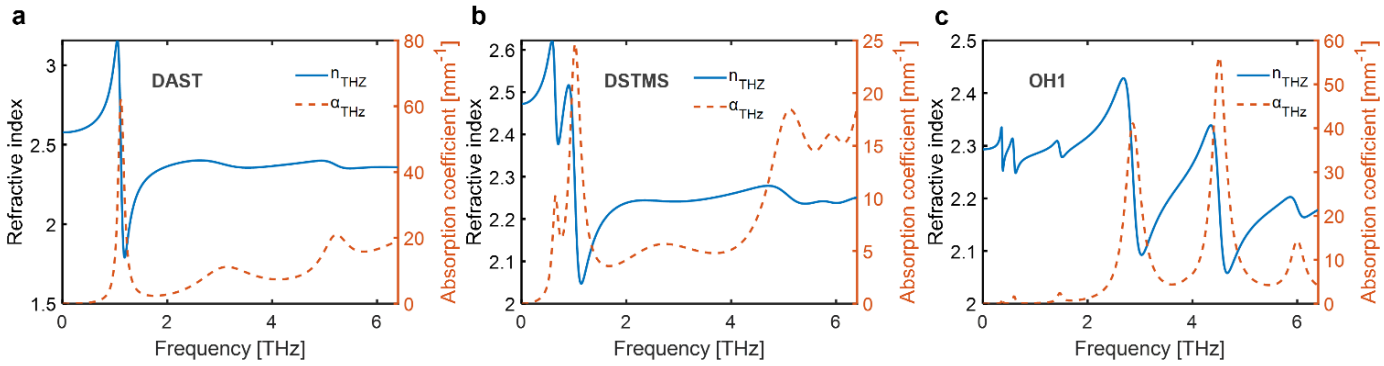

Fig. S4 Optical properties in the THz range. (a)-(c) The calculated refractive index and the absorption coefficient as a function of frequency in DAST, DSTMS along the *a*-axis, and OH1 along the *c*-axis.

SIII. Polarization dependence of SHG from DSTMS and OH1 crystals

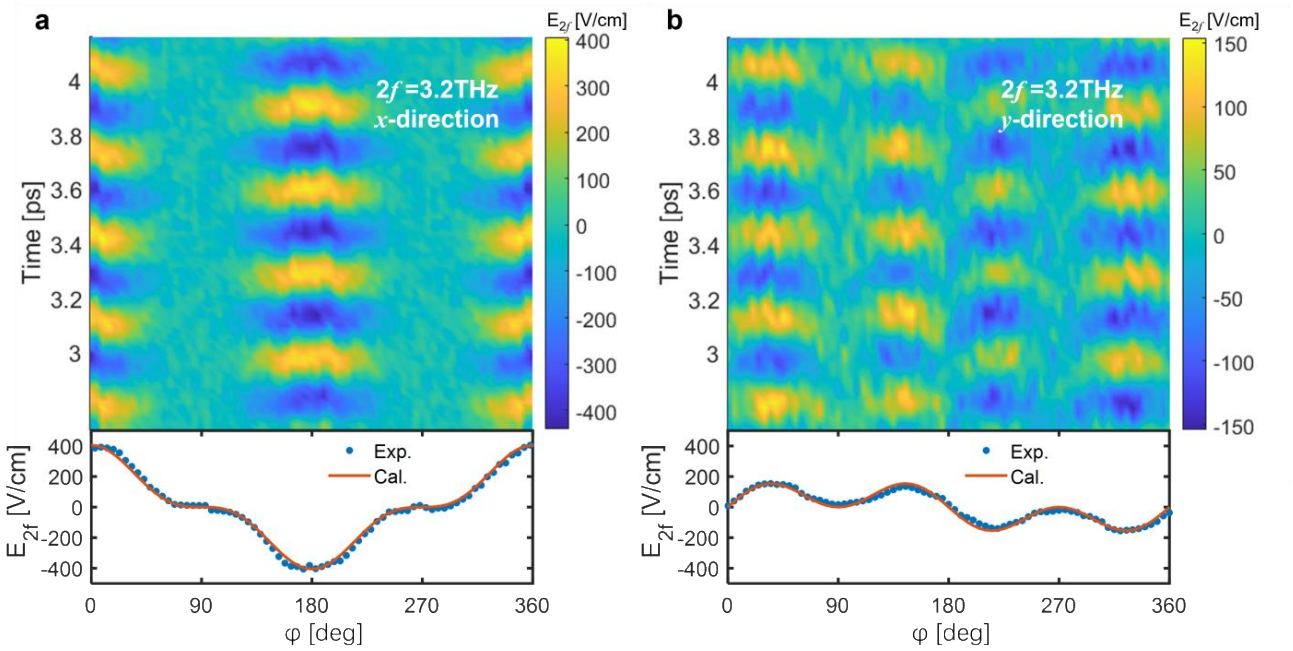

Fig. S5 Polarization dependence of SHG from DSTMS crystal with the pump frequency of 1.6 THz. (a)-(b) The measured time-domain waveform of SHG in the *x*- and *y*-direction with the DSTMS rotation angle of φ. The color information represents the electric field of SHG. The bottom panels of the figure represent the variation of the peak electric field of the SHG with the rotation angle of φ.

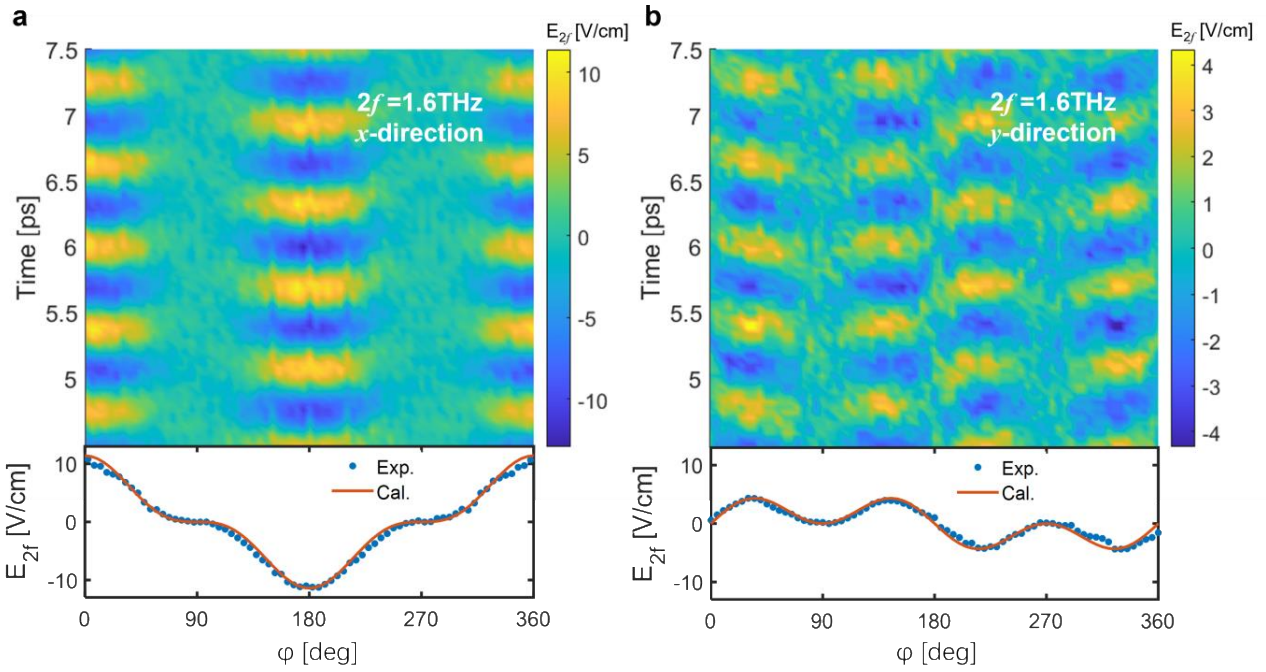

Fig. S6 Polarization dependence of SHG from OH1 crystal with the pump frequency of 0.8 THz. (a)-(b) The measured time-domain waveform of SHG in the x- and y-direction with the OH1 rotation angle of φ. The color information represents the electric field of SHG. The bottom panels of the figure represent the variation of the peak electric field of the SHG with the rotation angle of φ.

SIV. Stability measurement and error evaluation of SHG signals

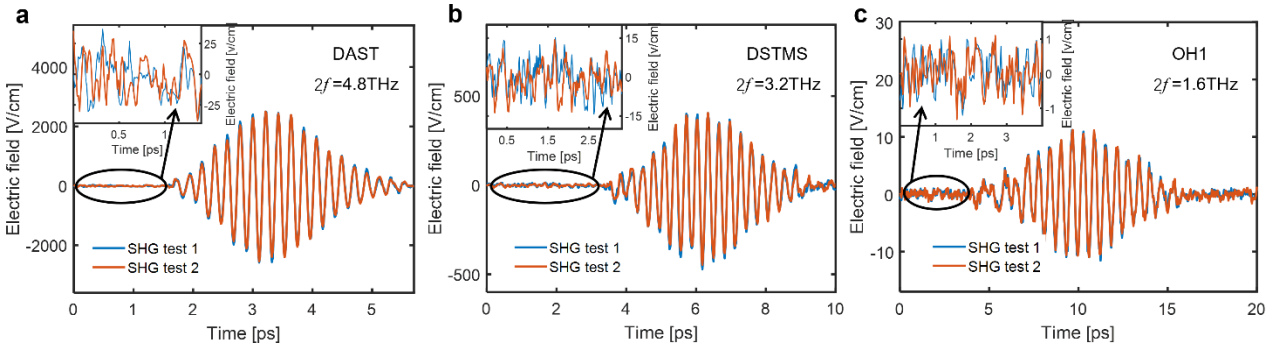

Fig. S7 Stability measurement for SHG. (a) Repeatability measurement of THz SHG from a DAST crystal with a fundamental frequency of 2.4 THz, and the inset shows the noise scale of the signal. (b) Repeatability measurement of THz SHG from a DSTMS crystal with a fundamental frequency of 1.6 THz, and the inset shows the noise scale of the signal. (c) Repeatability measurement of THz SHG from an OH1 crystal with a fundamental frequency of 0.8 THz, and the inset shows the noise scale of the signal.

Figure S7 shows the stability measurement for SHG. The insets in Figs. S7(a)-(c) show the fluctuation caused by background noise signals. This is also the main source of instability factors in repetitive measurements. Figure S7(a) shows the two measurements of the second harmonic waveform at a frequency of 4.8 THz detected by a 200 μm GaP crystal. The inset shows the noise level, which shows that the error range of the measurement is within ±25 V/cm. Figure S7(b) shows the two measurements of the second harmonic waveform at a frequency of 3.2 THz detected by a 200 μm GaP crystal, and its inset shows that the error range is within ±15 V/cm. Due to the higher responsiveness of GaP crystal to 3.2 THz compared to 4.8 THz, the error range shown in Fig. S7(b) is smaller than that in Fig. S7(a). Figure S7(c) shows the two measurements of the second harmonic waveform at a frequency of 1.6 THz detected by a 1 mm ZnTe crystal, and its inset shows that the error range is within ±1 V/cm.